



LBT & Image

# "X-RAY RESONANT IRRADIATION AND HIGH-Z RADIOSENSITIZATION IN CANCER THERAPY USING PLATINUM NANO-REAGENTS"

Sultana N. Nahar

Astronomy

Sara Lim (Biophysics, OSU), M. Montenegro  
(Catholic U. of Chile), A. K. Pradhan (Astronomy,  
OSU), R. BARTH (Pathology, OSU), E. Bell  
(Radiation Oncology, OSU), E. Chowdhury  
(Physics, OSU), C. Turro, Russ M. Pitzer  
(Chemistry, OSU)

*"67th International Symposium on  
Molecular Spectroscopy"*

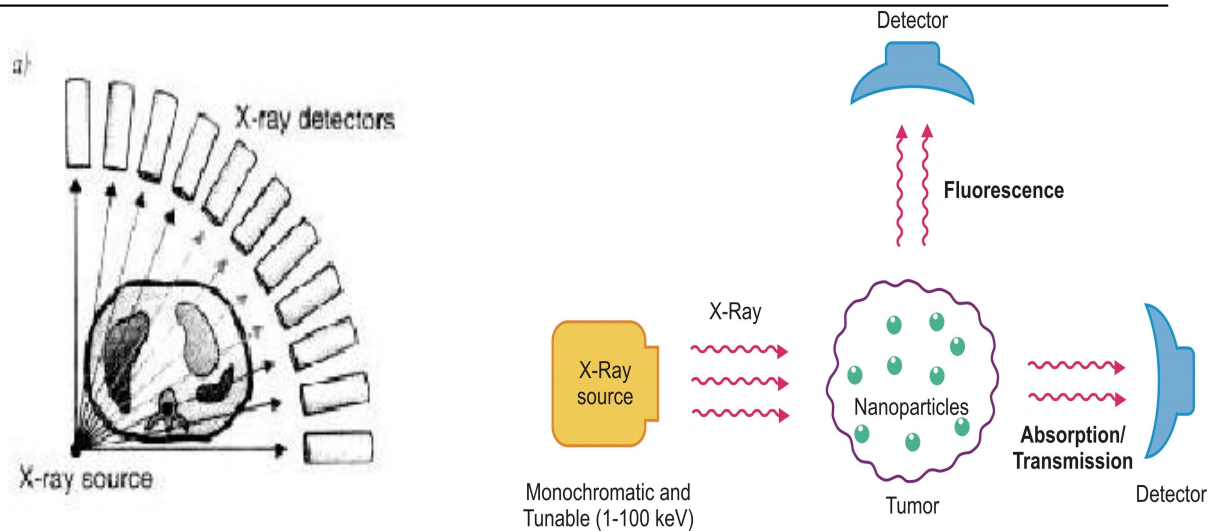
Ohio State University, Columbus, Ohio, USA

June 18-22, 2012

**Support:** DOE, NSF, Ohio Supercomputer Center

# RNPT METHOD FOR CANCER TREATMENT

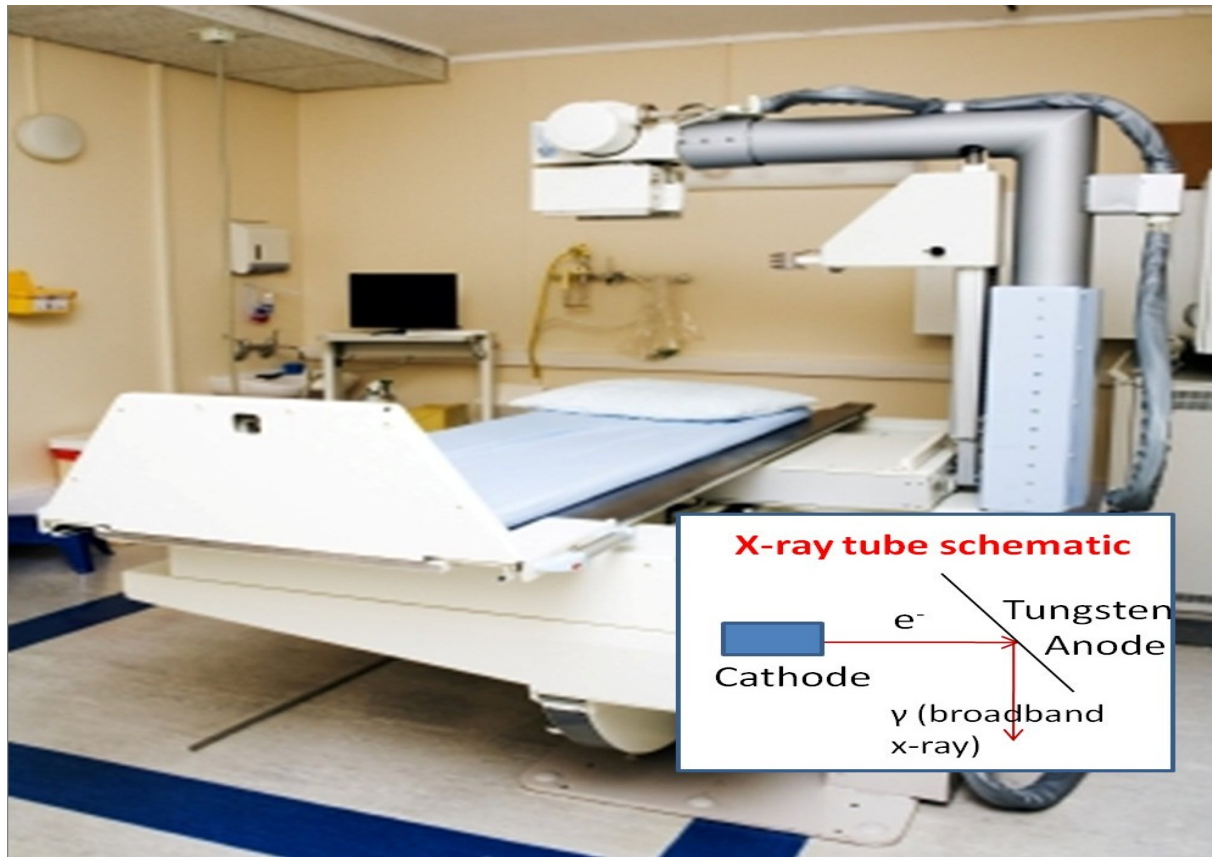
(Pradhan et al 2007, 2009)- Latest Progress:



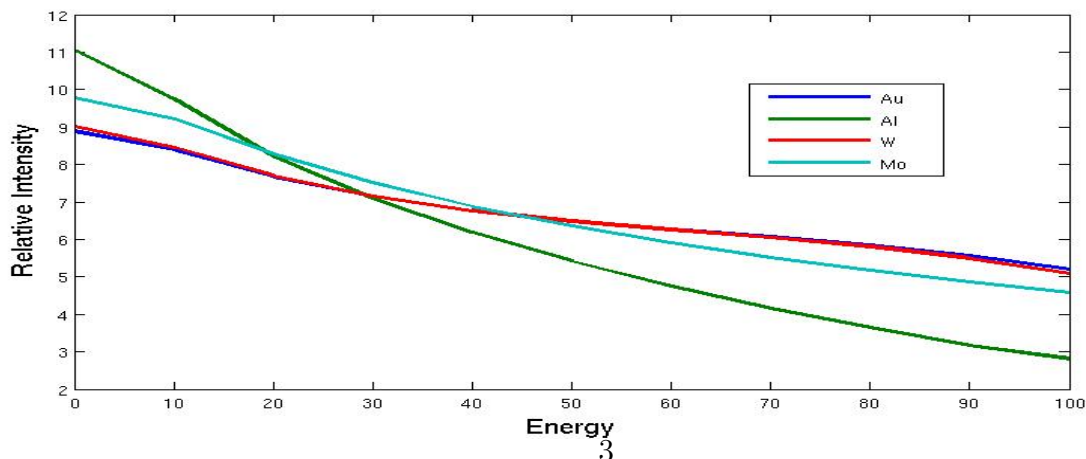
- Left: Full body CAT scans - use high energy broad band X-rays, very high radiation dosages
- Right: RNPT Method - Broadband imaging to Monochromatic Spectroscopy
- Spectroscopy: Accurate info, reduced exposure
- Nanoparticles (NP) are embeded in the tumor and are irradiadated by X-rays for inner shell absorptions leading to ejection of electrons and photons. Electrons breakup the DNA of the surrounding tumor cells - fluorescence to imaging
- Hence the method has several components
- **Need:** 1) a tunable monochromatic X-ray source
- 2) Heavy element and non- or low toxic NP for absorption of high energy X-rays that are transparent to biogenic elements (H,C,N,O,CHON)
- 3) X-rays at resonant energies of the nanoparticles

## X-RAY SOURCES IN MEDICAL FACILITIES

- Inset: An electron beam accelerates across  $\Delta V$  between the cathode and the anode, strikes a high-Z target (e.g. W,  $Z=74$ ), produces bremsstrahlung radiation of energy from zero to the peak voltage as they decelerate;

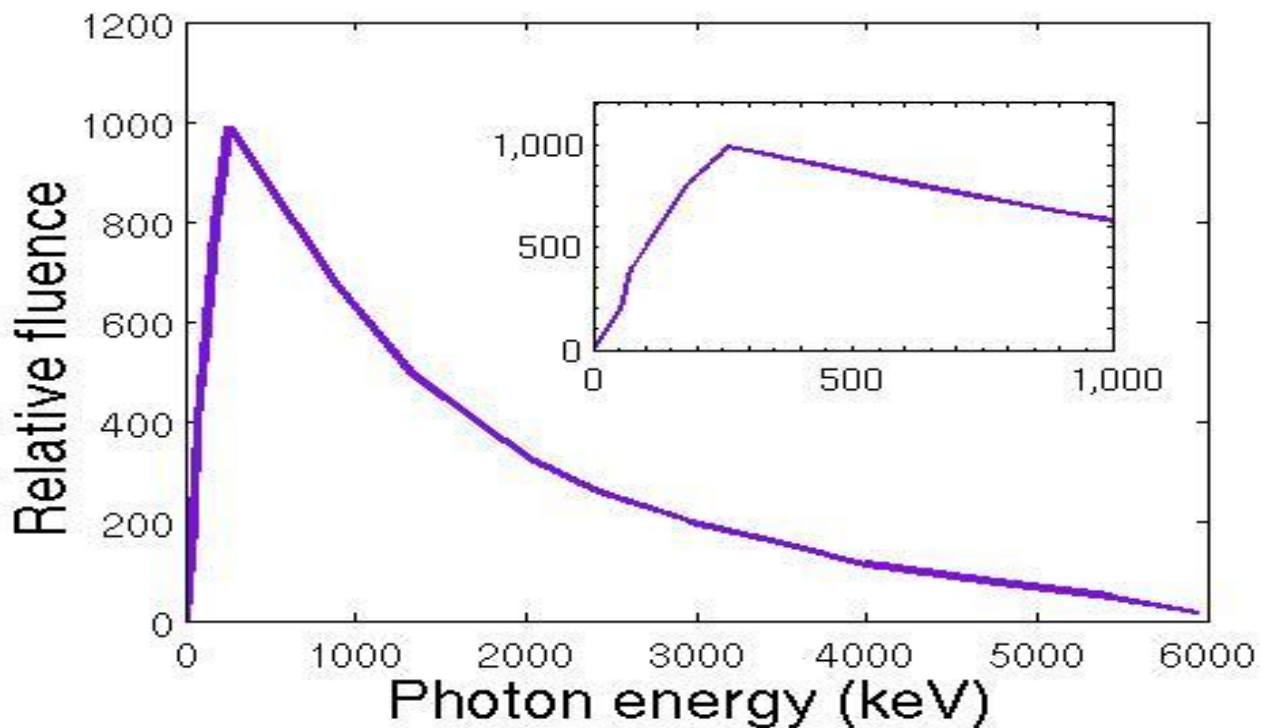
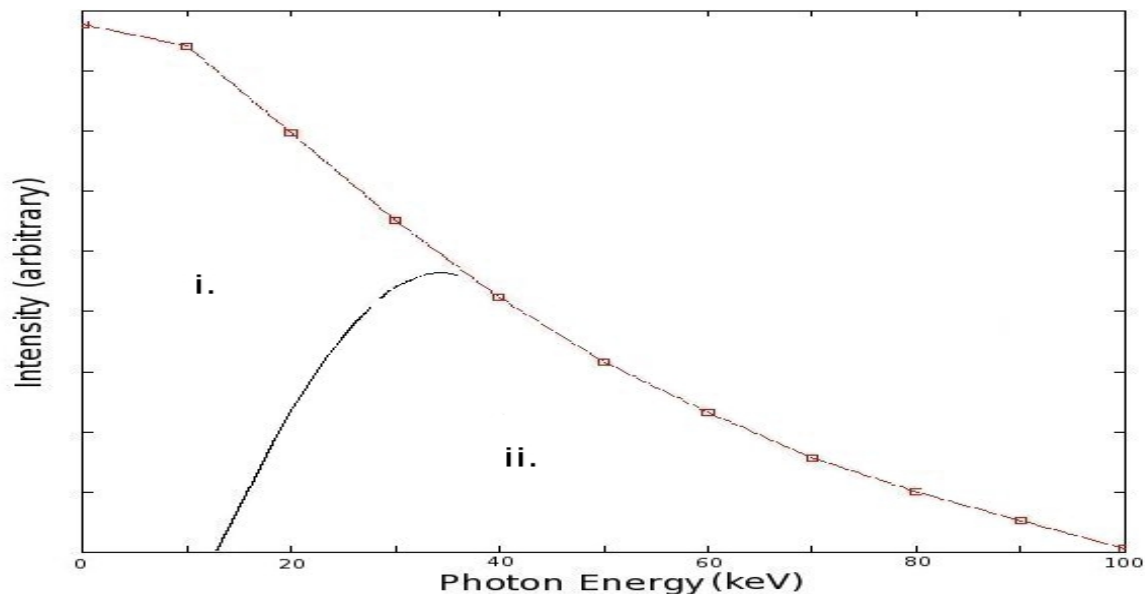


- Fig: Bremsstrahlung: Al (green), Mo (turquoise) W(red), Au (blue)



## Filtered Bremsstrahlung of an X-ray Machine

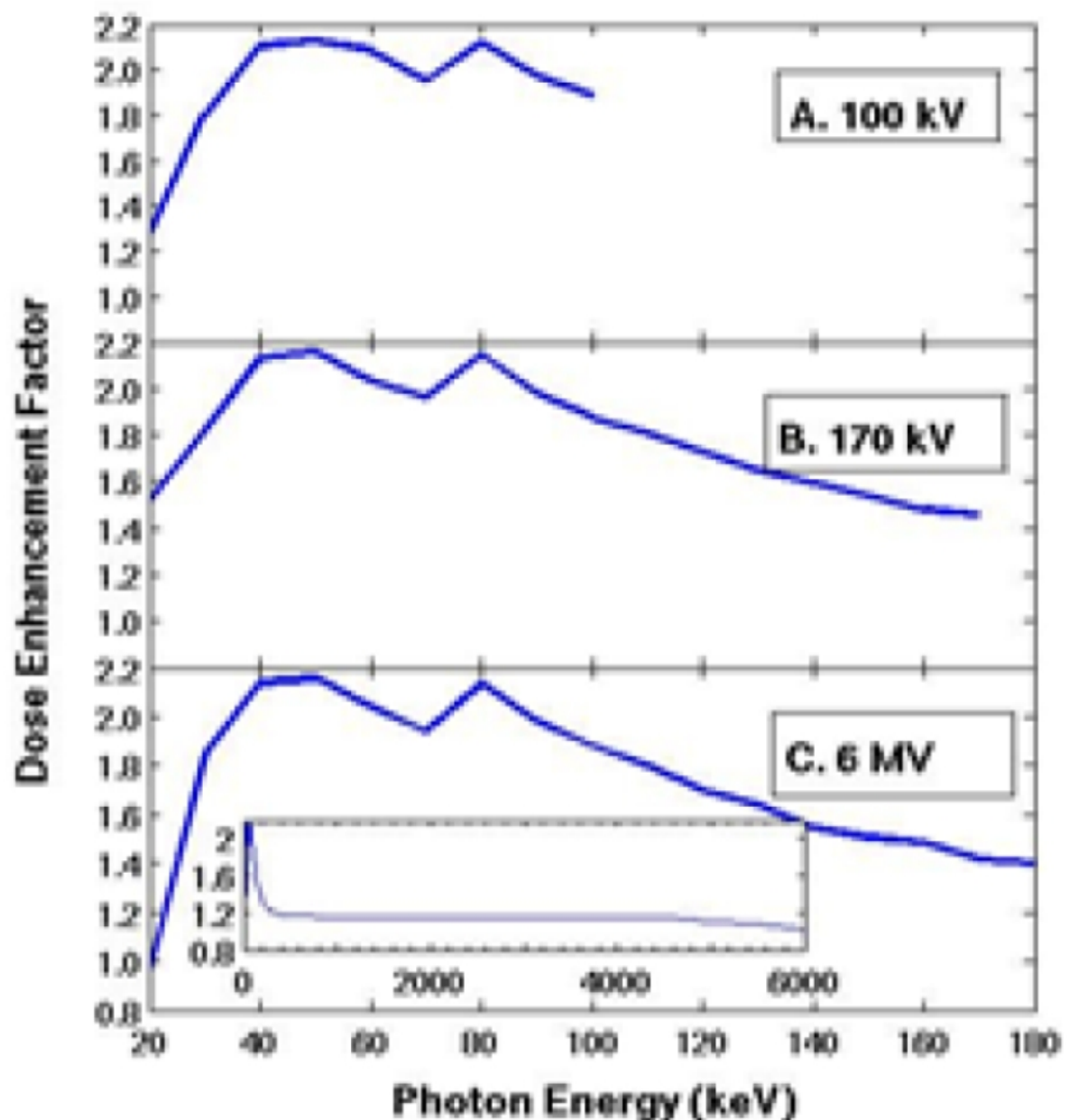
- A filter (e.g. Al, dotted) - reduces the harmful low energy radiation
- Bremsstrahlung Max at  $\sim 1/3$  of kVP or MVp
- Fig: Bremsstrahlung with W target & Al filter



- Bremsstrahlung from a 6 MeV LICAC with a peak around 300 keV from filtering the lower energy x-rays

## X-RAY ABSORPTION & DOSE DEPOSITION OF Pt

- Fig: Monte Carlo Simulation of x-ray dose deposition (Dose Enhancement Factor DEF) in tissues with Pt  
X-ray sources: 100 keV, 170 keV, 6 MeV broadband X-ray sources - 100 keV is efficient (Lim et al 2012)
- DEF: 1st peak ( $\sim 40$  keV)- L-shell ionization, 2nd peak ( $\sim 80$  keV - K-shell ionization. Then decays (no more ionization threshold - largely Compton scattering)

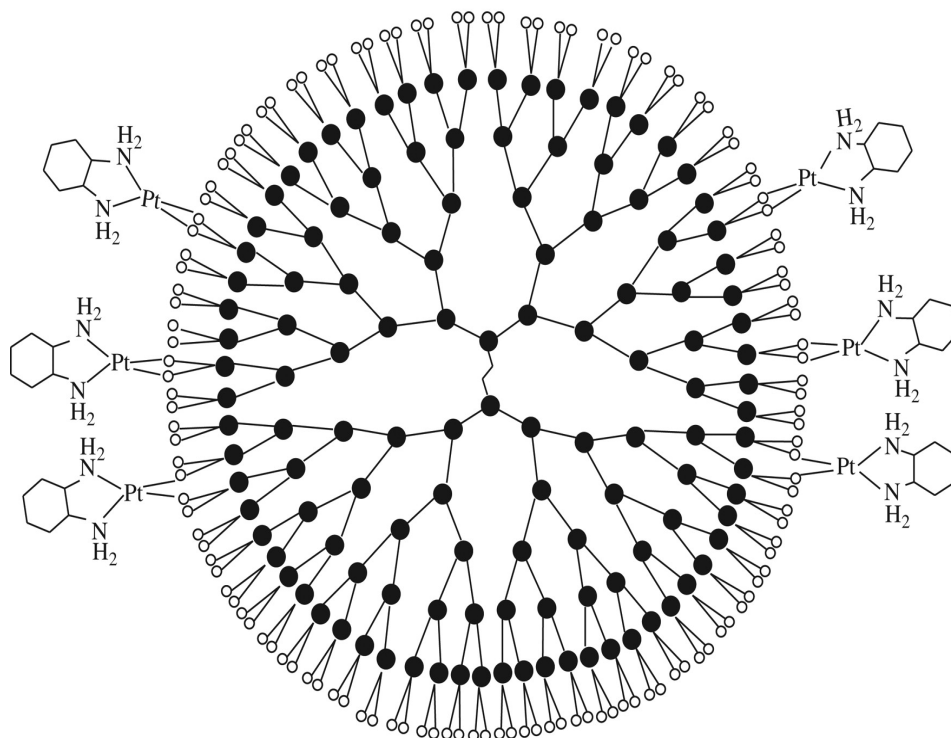
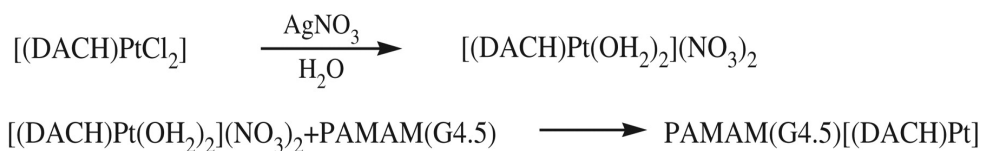




## NP: PLATINATED DENDRIMERS

- Dendrimer - a delivery vehicle for anticancer drugs; a solution to lowering toxicity of organoplatinum drugs
- Can have tunable layers (generations) of structure allowing encapsulation or conjugation of multiple entities either in the core or on the surface
- Have identified an effective conjugate platinated dendrimer - water soluble, low toxicity

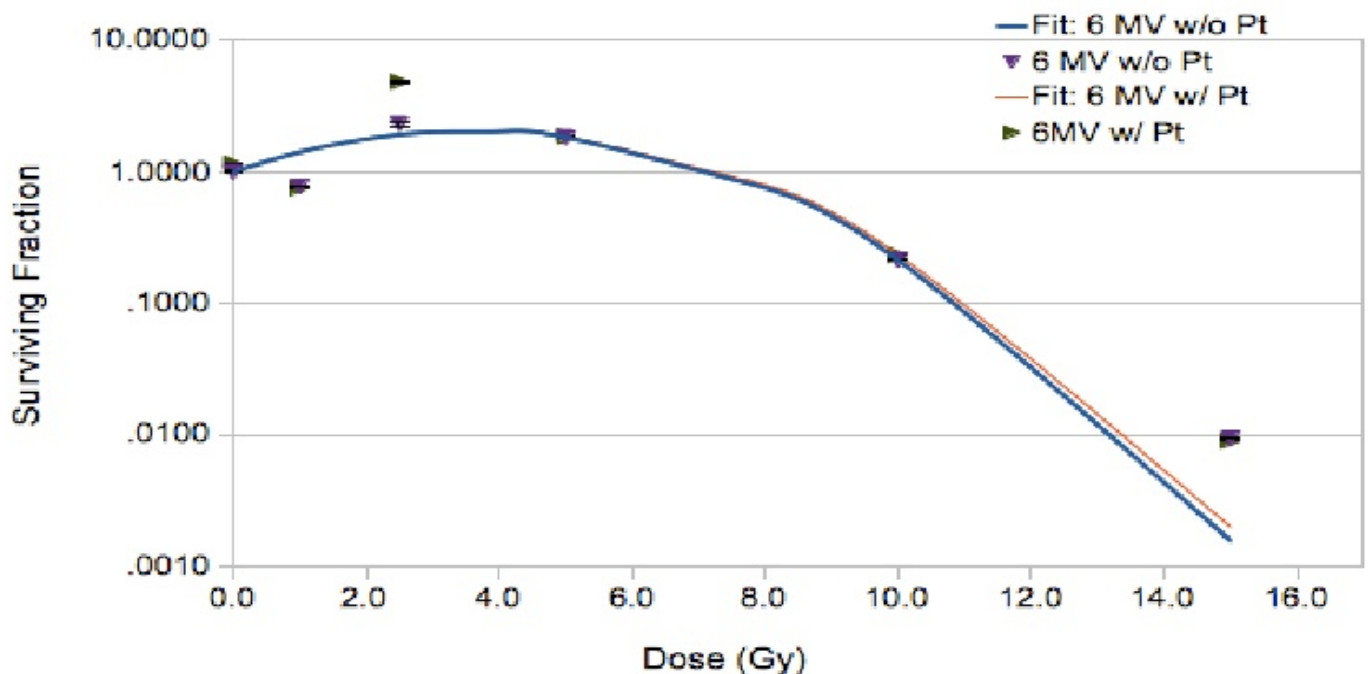
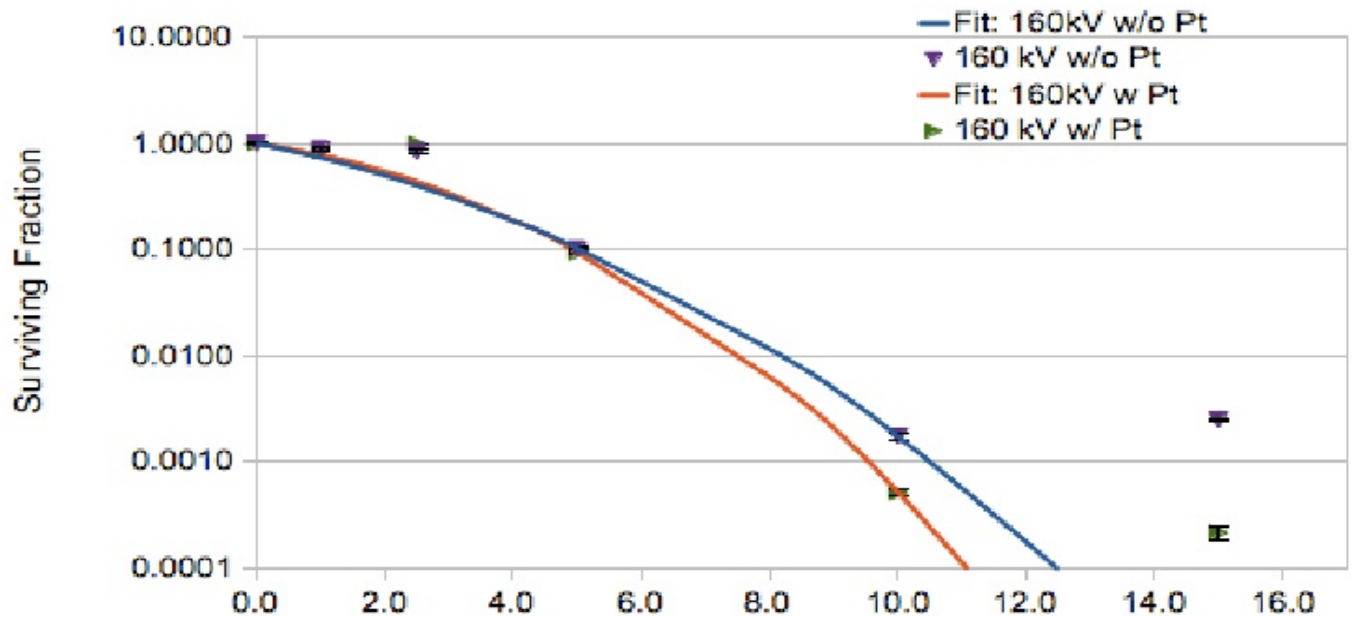
Synthesis of PAMAM(G4.5)-[(DACH)Pt] nanoconjugate and a diagram of its structure (other [(DACH)Pt] units omitted for clarity).



Howell B A , Fan D Proc. R. Soc. A 2010;466:1515-1526

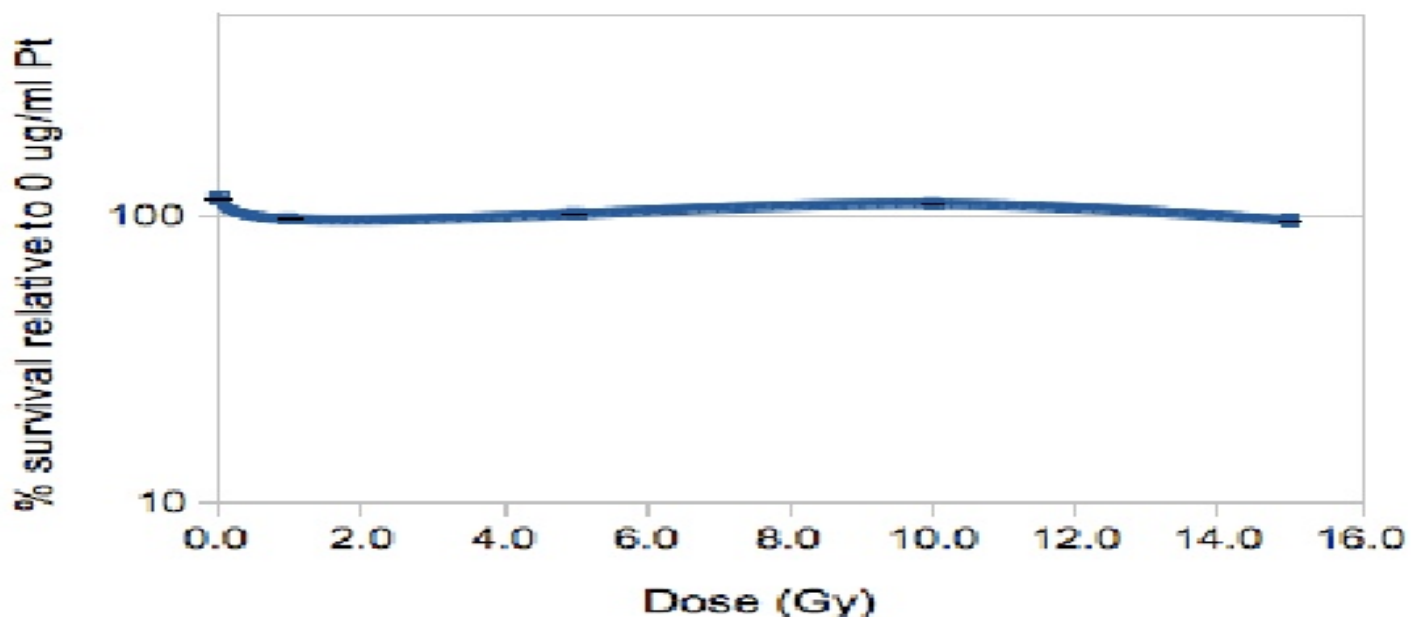
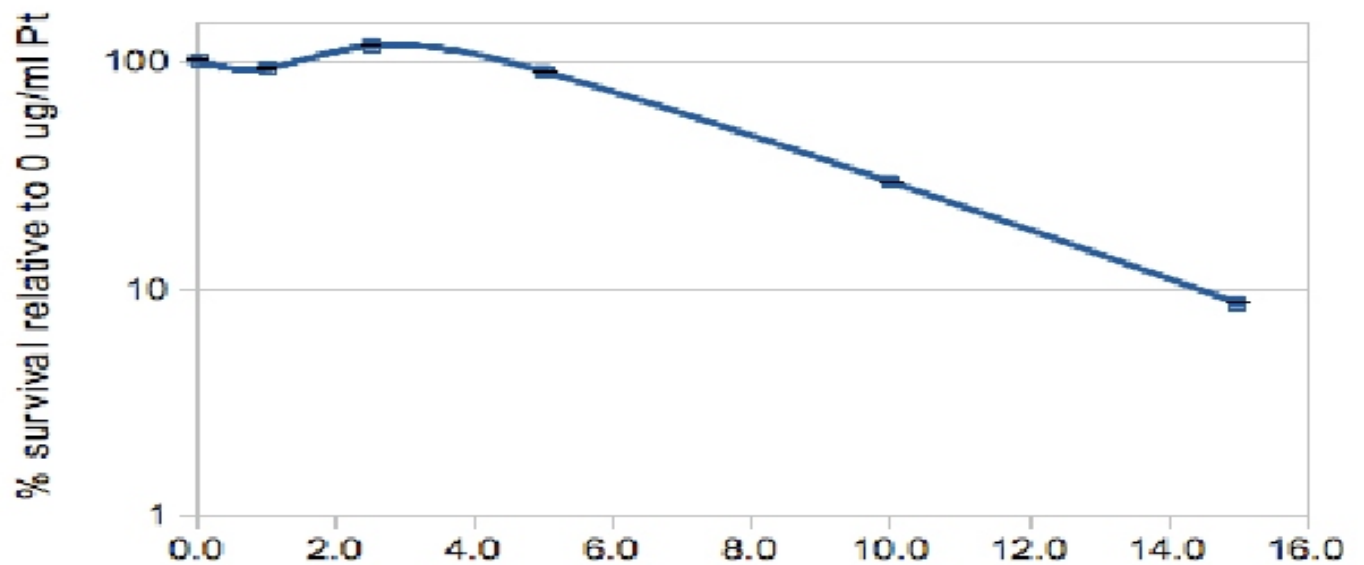
## RNPT EXPERIMENT: SURVIVAL OF CANCER CELL (Mouse):

- Study of X-ray energy effect on survival of cultured mouse cancer cells with platinate dendrimers
- X-ray source - Top: 160 keV, Bottom: 6 MeV



## RNPT EXPERIMENT: CANCER CELL SURVIVING FACTOR:

- 160 keV X-rays - surviving factor (SF) goes down with lower energy, 6 MeV X-rays - SF remains constant
- Top: 160 keV, Bottom: 6 MeV





## X-RAY INTERACTION WITH NANOPARTICLES and Relevant Atomic Parameters

### 1. Photoexcitation:

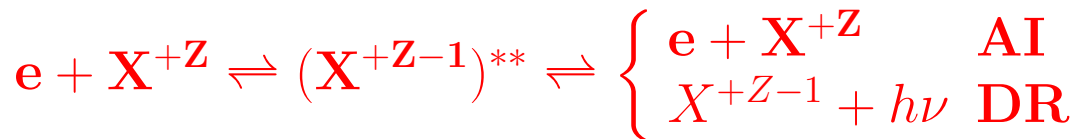


- Oscillator Strength ( $f$ ), Radiative Decay Rate ( $A$ -value)

### 2. Direct Photoionization (PI) :



### 3. Photoionization via an Autoionizing State :



*The doubly excited state - "autoionizing state" - introduces resonances*

- 2 & 3. Photoionization Cross Sections ( $\sigma_{PI}$ )

## THEORY

For a multi-electron system, in nonrelativistic LS coupling:

$$\mathbf{H}^{\text{NR}}\Psi = \left[ \sum_{i=1}^N \left\{ -\nabla_i^2 - \frac{2Z}{r_i} + \sum_{j>i}^N \frac{2}{r_{ij}} \right\} \right] \Psi = \mathbf{E}\Psi. \quad (1)$$

**Relativistic effects:** For a multi-electron system, the Breit-Pauli Hamiltonian is:

$$\mathbf{H}_{\text{BP}} = \mathbf{H}_{\text{NR}} + \mathbf{H}_{\text{mass}} + \mathbf{H}_{\text{Dar}} + \mathbf{H}_{\text{so}} + \frac{1}{2} \sum_{i \neq j}^N [\mathbf{g}_{ij}(\mathbf{so} + \mathbf{so}') + \mathbf{g}_{ij}(\mathbf{ss}') + \mathbf{g}_{ij}(\mathbf{css}') + \mathbf{g}_{ij}(\mathbf{d}) + \mathbf{g}_{ij}(\mathbf{oo}')]. \quad (2)$$

where the Breit interaction is

$$\mathbf{H}^{\text{B}} = \frac{1}{2} \sum_{i>j} [\mathbf{g}_{ij}(\mathbf{so} + \mathbf{so}') + \mathbf{g}_{ij}(\mathbf{ss}')] \quad (3)$$

and one-body corrections terms are

$$\mathbf{H}^{\text{mass}} = -\frac{\alpha^2}{4} \sum_i \mathbf{p}_i^4, \quad \mathbf{H}^{\text{Dar}} = \frac{\alpha^2}{4} \sum_i \nabla^2 \left( \frac{Z}{r_i} \right), \quad \mathbf{H}^{\text{so}} = \left[ \frac{Ze^2\hbar^2}{2m^2c^2r^3} \right] \mathbf{L} \cdot \mathbf{S}$$

## ATOMIC PROCESSES:

**Transition Matrix elements with dipole operator  $\mathbf{D} = \sum_i \mathbf{r}_i$ ,**

$\langle \Psi_B || \mathbf{D} || \Psi_{B'} \rangle \rightarrow$  **Radiative Excitation and Deexcitation**

$\langle \Psi_B || \mathbf{D} || \Psi_F \rangle \rightarrow$  **Photoionization and Recombination**

$\mathbf{D} = \sum_i \mathbf{r}_i \rightarrow$  Dipole Operator

The matrix element reduces to generalized line strength,

$$\mathbf{S} = \left| \left\langle \Psi_f \left| \sum_{j=1}^{N+1} \mathbf{r}_j \right| \Psi_i \right\rangle \right|^2 \quad (4)$$

### Oscillator Strength. Cross Section, Attenuation Coefficient

• The oscillator strength ( $f_{ij}$ ) and radiative decay rate ( $A_{ji}$ ) for the bound-bound transition are

$$f_{ij} = \left[ \frac{E_{ji}}{3g_i} \right] S, \quad A_{ji}(\text{sec}^{-1}) = \left[ 0.8032 \times 10^{10} \frac{E_{ji}^3}{3g_j} \right] S \quad (5)$$

Employing the calculated transition rates for the  $K\alpha$  resonances, we compute the resonant photoabsorption cross sections

$$\sigma_{K\alpha}(\nu; \mathbf{K} \rightarrow \mathbf{L}_i) = \frac{4\pi^2 a_o^2 \alpha}{3} \frac{E(\mathbf{K} - \mathbf{L}_i)}{g_k} S(\mathbf{K} - \mathbf{L}_i) \phi(\nu) \quad (6)$$

where the  $L_i$  refers to the upper level in the open (ionized) L-shell,  $E(K - L_i)$  is the corresponding energy, and  $S(K - L_i)$  is the line strength, and the initial level statistical weight  $g_K = 1$ .

• We are interested in photoionization of K-shell to initiate Auger process for multiple electron and photon productions

## Auger Cascade: ELECTRON & PHOTON EMISSIONS

- Fig (i) Photoionization by X-ray photons ( $E_X$ ) ( $>$  K-shell ionization energy  $E_K$ ) leading to Auger process:  
A higher level electron drops to fill a lower level vacancy, but emits a photon that can knock out another electron.
- Fig (ii) Multiple electron vacancies due to successive Auger decays lead to cascade of photon and electron emissions
- Single ionization of 1s electron can lead to ejection of 20 or more electrons in an ion with occupied O and P shells
- Fig (iii) Inverse to Auger - Resonant photo-excitation from  $1s \rightarrow 2p$  (with L-shell vacancy) by an external monoenergetic X-ray source with intensity above our predicted critical flux (Pradhan et al 2009):

$$\Phi^c(\nu_{K\alpha}) = \frac{\sum_{n_i \geq 2} g_i A[n_i(S_i L_i J_i) \rightarrow 2(SLJ)]}{g_K B_{K\alpha}}. \quad (7)$$

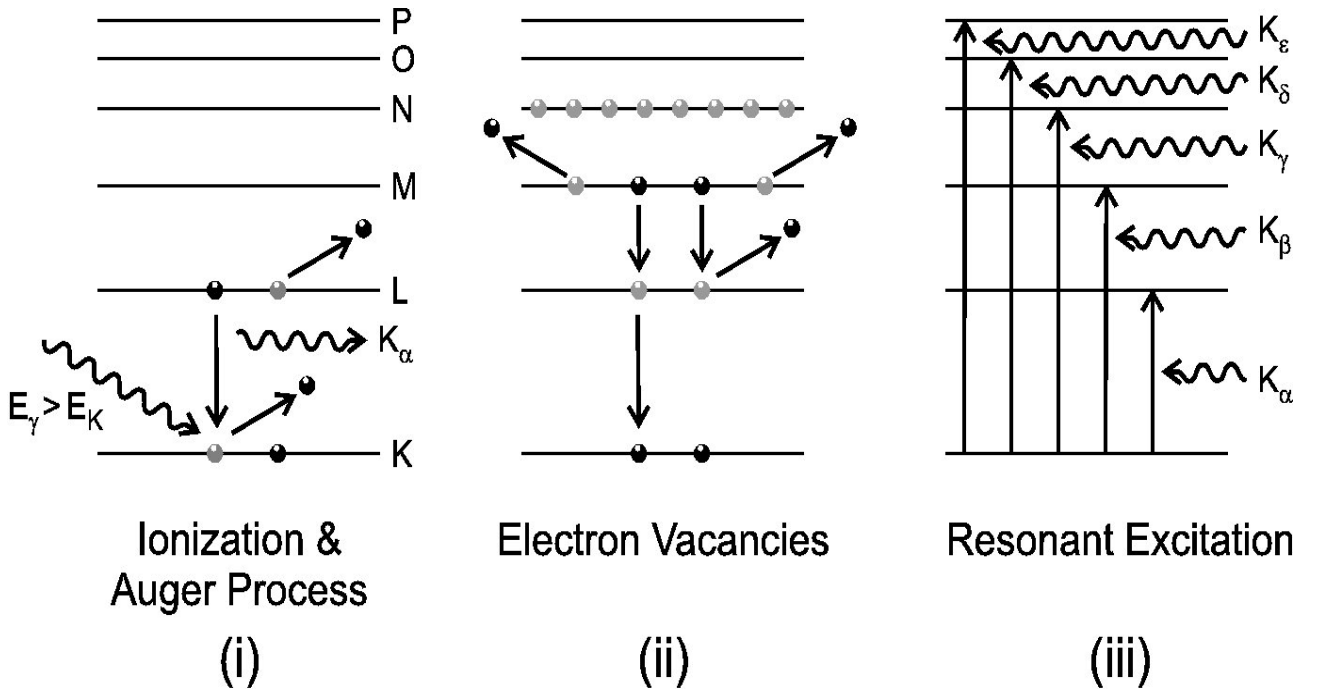


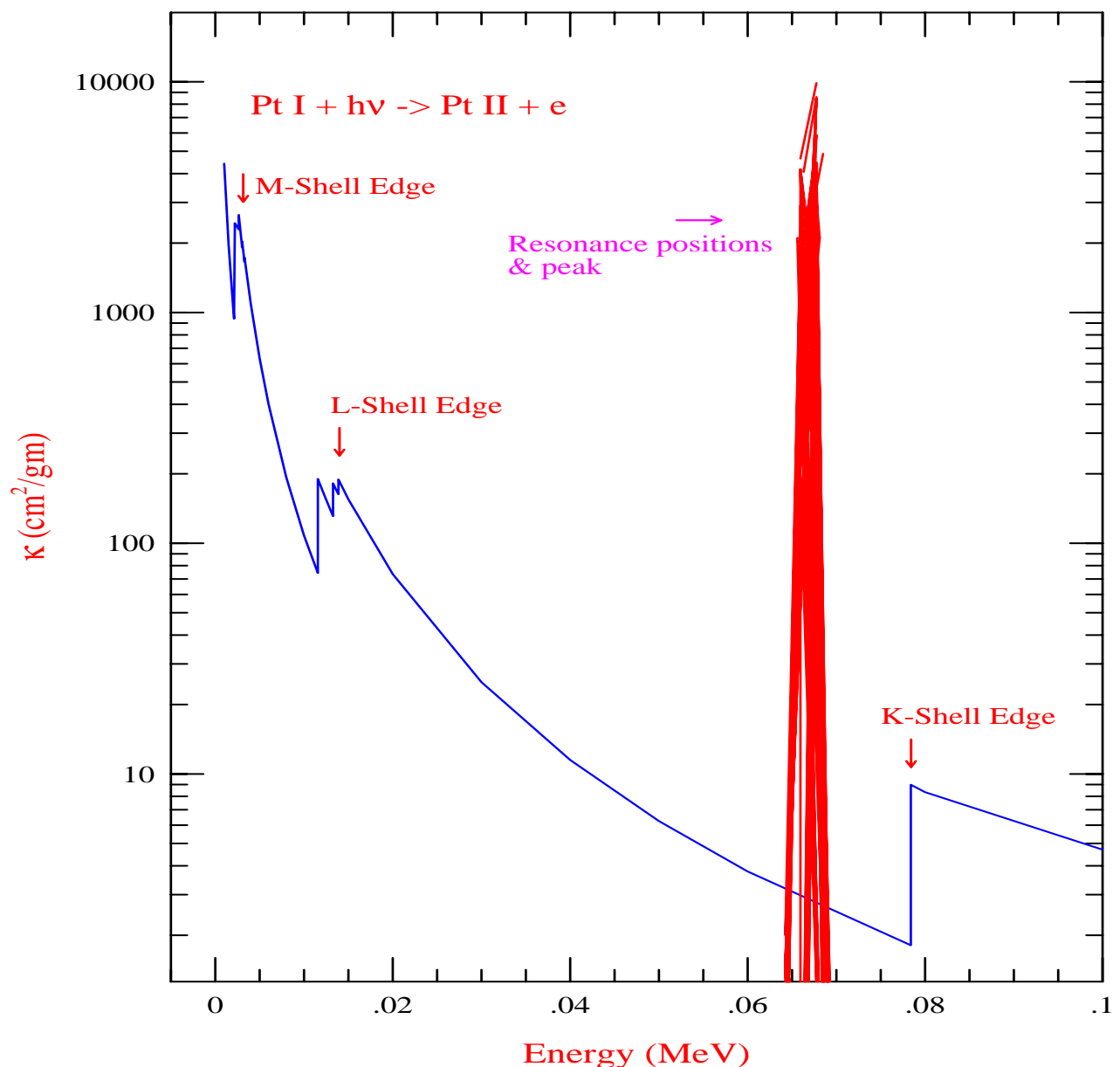
## Photo-Absorption Coefficient $\kappa(\text{cm}^2/\text{g})$ :

$\text{Pt} + h\nu \rightarrow \text{Pt}^+ + \text{e}$  (Nahar et al 2011)

- Blue curve: Background  $\kappa$ , Red: Resonances below K-edge
- Enhancements in  $\kappa \rightarrow$  at K, L, M (sub)-shells ionization
- Rise at  $E_K$ , focus of experiments but without success,
- K- $\alpha$  resonances (red), due to  $\text{K} \rightarrow \text{L}$  excitations, are in  $E_{\text{res}} = 64 - 70 \text{ keV}$ , below  $E_K$

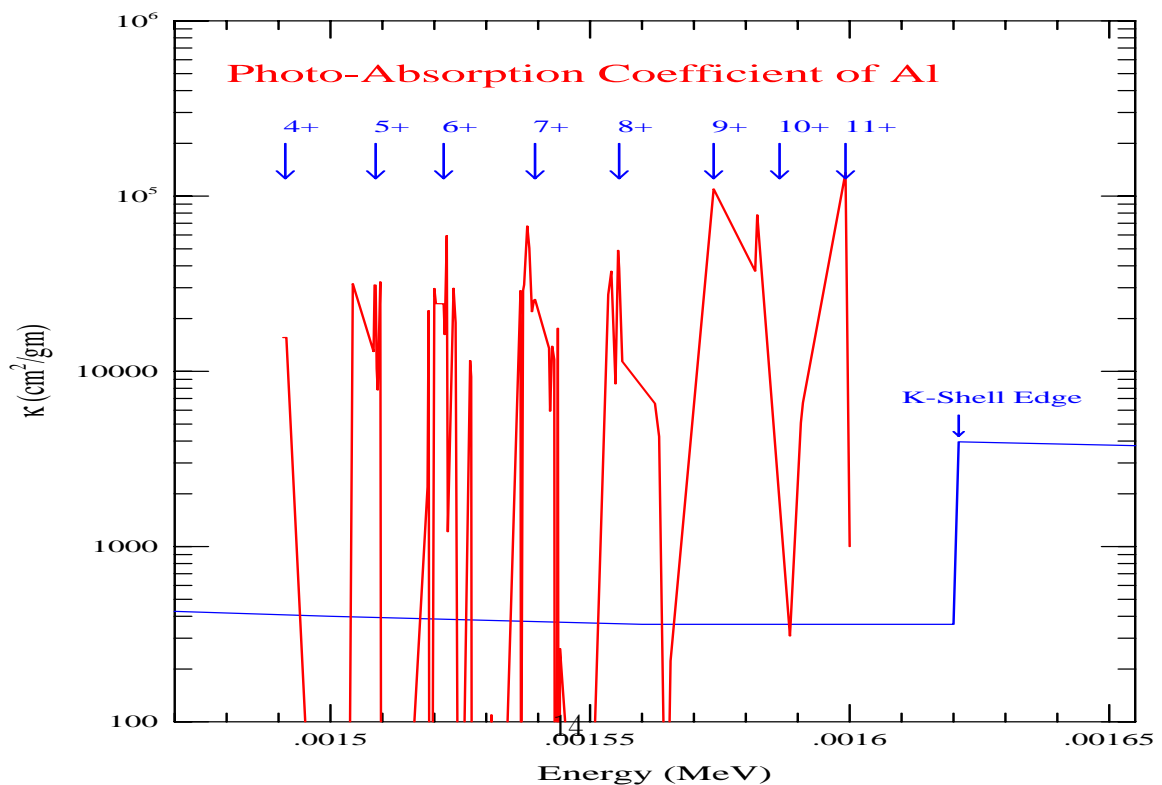
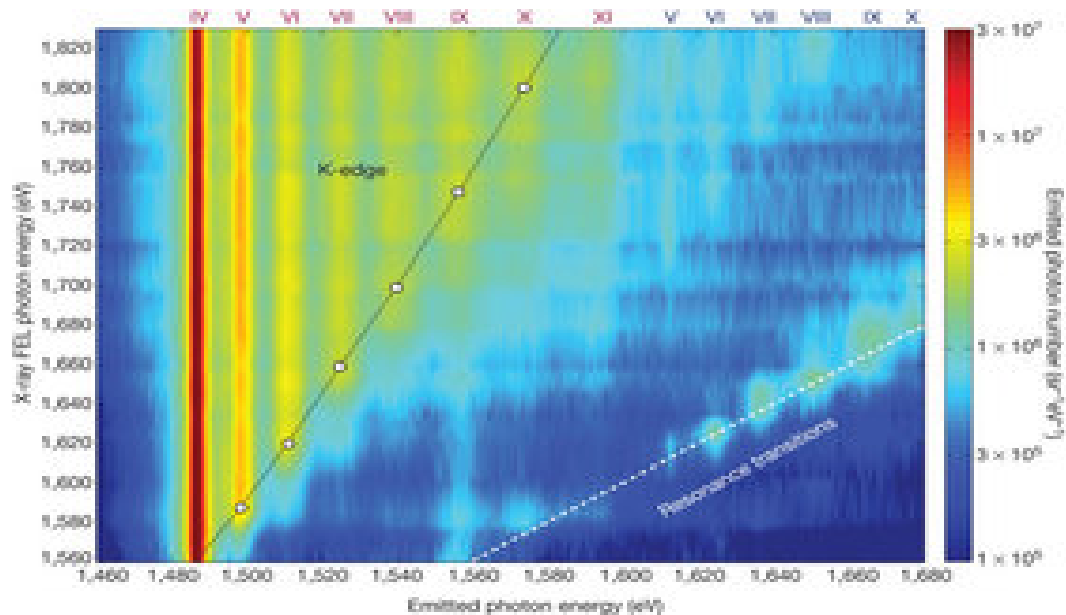
$\rightarrow$  Will increase in ejected electrons in  $E_{\text{res}}$

### Photo-Absorption Coefficient of Platinum



# Resonant $K_{\alpha}$ Emission Below K-Edge from Various Ionization States of Al

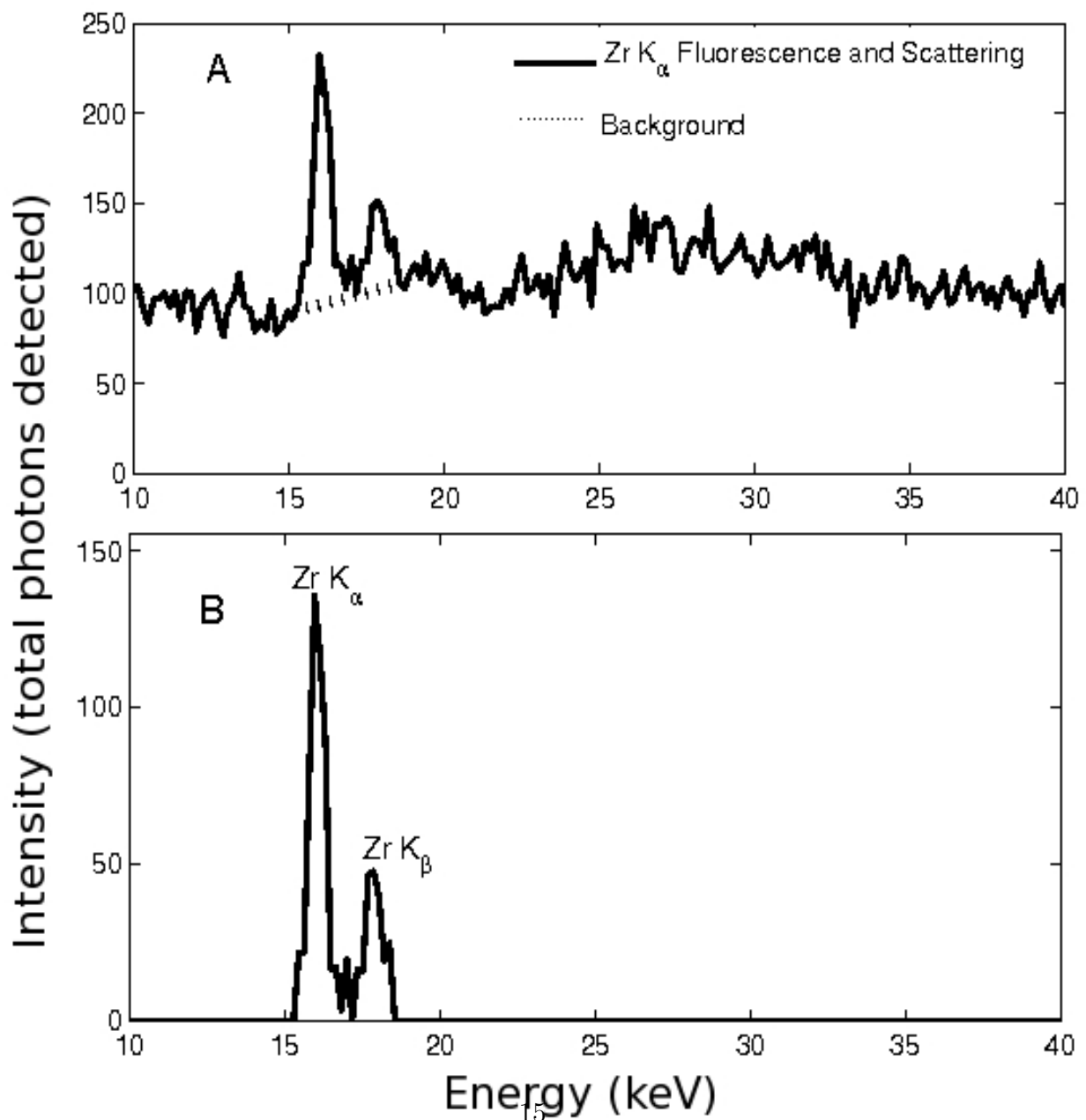
- Top: Berkeley Experiment (Vinko et al, Nature Lett 2012)
- Detected  $K_{\alpha}$  photons at 1.46-1.68 keV below K-edge
- $K_{\alpha}$  resonances predicted for gold (Pradhan et al. 2009)
- Bottom: Predicted  $K_{\alpha}$  resonances (red) (Blue: background)





## Production of Monochromatic X-rays

- Monochromatic radiation, such as,  $K_\alpha$  can be produced by directing the bremsstrahlung, of flux distribution  $f_B$ , to a high-Z target (X), rotated at a selective angle
- Inner K-shell ionization in the target followed by radiative decays by upper shell electrons can produce X-ray fluorescence at monochromatic energies.
- Figure: Production of  $K_\alpha$  X-rays from Zr 100 keV bremsstrahlung (Lim et al 2012)



## Flourescence Yield & Intensity of the Monochromatic Beam

- The K-flourescence yield ( $\omega_K$ ) can be estimated from the branching ratio:

$$\omega_K = \frac{A_r(L - K)}{[A_r(L - K) + A_a(L)]}$$

$A_r(L - K)$  = Radiative decay rate for ( $L \rightarrow K$ ),  $A_a$  = Autoionization decay rate. For high-Z elements, e.g. Pt,  $\omega_K > 0.95$

→ All photons from the Bremsstrahlung source above the K-shell ionization energy,  $E > E_K$ , may be converted into monochromatic  $K_\alpha$  radiation with high efficiency

- The estimated intensity of the monochromatic energy:

$$I(K_\alpha) \sim N(X) \int_{E \geq E_K}^{E(kVp)} f_B \sigma_K(E) dE$$

$N(X)$  = number density,  $\sigma_K$  = K-shell photoionization cross section. For Zr: Efficiency of conversion  $\sim 2$

- The K-flourescence yield ( $\omega_K$ ) in general produces weaker beam intensity
- However, for high-Z elements,  $\omega_K \sim 1$
- Our effort on producing monochromatic X-rays is continuing

## CONCLUSION

1. We present progress on our multidisciplinary program on RNPT
2. Demonstrated effective energy range for X-rays in the medical X-ray sources
3. Presented preliminary results on killing cancer cells using RNPT method
4. Demonstrated the resonant energies for Pt and Al for effective Auger process
5. Current status on producing monochromatic X-rays